Journal of Engineering and Applied Sciences 11 (4): 920-929, 2016
ISSN: 1816-949X

Free Vibration Analysis of Sandwich Cylindrical Panel with Functionally Graded Core by Using ABAQUS Software

[1]M. Garooschi and [2]F. Barati
[1]Department of Mechanics, Faculty of Engineering, Islamic Azad University, Hamedan Science and Research Branch, Hamedan, Iran
[2]Department of Mechanical Engineering, Islamic Azad University, Hamedan Branch, Hamedan, Iran

Abstract: This study presents an exact three-dimensional free vibration solution for sandwich cylindrical panels with functionally graded core. Material properties of the FGM core are assumed to be graded in the radial direction, according to a simple power-law distribution in terms of volume fractions of the constituents. Poisson's ratio is assumed to be constant. The governing equation of motions is formulated based on the 3D-theory of elasticity and displacement fields are expanded in Fourier series along the in-plane coordinates which satisfy the simply supported edges boundary conditions. The state space technique is used to obtain natural frequencies analytically. Accuracy and convergence of the present approach are examined by comparing the analytical results with the existing values in literature. The parametric study is carried out to discuss the effects of gradient index, geometrical properties such as span angle, facing layers thickness and axial length to mid radius ratio on the frequency behavior of the sandwich panel. The obtained exact solution shows that the FGM core has significant effects on the vibration behavior of sandwich cylindrical panel. This fist known exact solution serves as a benchmark for assessing the validity of numerical methods or two-dimensional theories used to analyses of sandwich cylindrical panels.

Key words: Free vibration, FGM, sandwich panel, 3D elasticity, state space

INTRODUCTION

Sandwich panels are important structural elements for many fields of lightweight construction. In conventional sandwich structures, due to the difference between stiffness of the face sheets and the core layer, debonding failure may occur at the interfaces. By using FGM core, resistance of sandwich panels to this type of failure increases. In recent years, static and free vibration behavior of sandwich panel has been extensively studied by some researchers. Gipson (1989) carried out frequency analysis of vibrating sandwich panels with directionally reinforced laminations. Based on the principle of virtual work (Xia and Lukasiewicz, 1995) analyzed free vibration of viscoelastic, damped sandwich cylindrical panel using the Runge-Kutta method. Free vibration analysis of doubly curved open deep sandwich shells was presented by Singh (1999) using the Rayleigh-Ritz method. Nonlinear free vibration of shallow asymmetrical, doubly curved sandwich shell with orthotropic core having different elastic characteristics was presented by Chakrabarti and Bera (2002). Khare *et al.* (2004) used the higher-order shear deformation theory and finite element method to study the free vibration behavior of isotropic, orthotropic and layered anisotropic composite and sandwich laminates. Kashtalyan and Menshykova (2009) investigated elastic deformation of sandwich panels with functionally graded core. Based on two dimensional theory (Moreira and Rodrigues, 2010) carried out static and dynamic analyses of sandwich panel using the finite element method. Rahmani *et al.* (2010) discussed free vibration of composite sandwich cylindrical shell with flexible core using the classical shell theory for the face sheets and elasticity theory for the core layer. Based on the refined three-layered theory (Biglari and Jafari, 2010) investigated free vibration of doubly-curved sandwich panels with flexible core. Rhmani *et al.* (2010) discussed free vibration of composite sandwich cylindrical shell with flexible core using the higher order sandwich panel theory. Effect of continuously grading fiber orientation face sheets on vibration behavior of sandwich panels with functionally graded core was studied by Aragh and Yas (2011) using the Generalized Differential Quadrature (GDQ) method. Mohammadi and Sedaghti (2012) analyzed free vibration of sandwich cylindrical shell with viscoelastic core using the semi-analytical finite element

Corresponding Author: M. Garooschi, Department of Mechanics, Faculty of Engineering, Islamic Azad University, Hamedan Science and Research Branch, Hamedan, Iran

method. Based on the Higher Order Zigzag Theory (HOZT), Kumar *et al.* (2013) analyzed free vibration behavior of laminated composite and sandwich shells using the 2D finite element method. Sobhy (2013) investigated vibration and buckling behavior of FGM sandwich plate resting on elastic foundations with various boundary conditions. Yas *et al.* (2013) discussed free vibration behavior of functionally graded nanocomposite cylindrical panels reinforced by single-walled carbon nanotubes using the theory of elasticity and generalized differential quadrature method. Dozio (2013) used two-dimensional Ritz method to investigate free vibration behavior of sandwich plate with FGM core layer. By using quasi-3D higher order shear deformation and a meshless technique, static, free vibration and buckling analysis of isotropic and functionally graded sandwich plates was discussed by Neves *et al.* (2013). Based on three-dimensional theory of elasticity, researcher analyzed free vibration behavior of nanoplate, cylindrical shell and cylindrical panel (Alibeigloo and Kani, 2010; Alibeigloo, 2011, 2012; Alibeigloo *et al.*, 2012). Recently, researcher (Alibeigloo, 2014) used theory of elasticity to carry out free vibration analysis of functionally graded carbon nanotube reinforced composite cylindrical panel embedded in piezoelectric layers. To our knowledge, three-dimensional free vibration solution of simply supported sandwich FGM cylindrical panel has not yet been investigated. Therefore, this first known solution provides an important benchmark for future assessing the validity of newly developed numerical methods such as meshless methods (Zhang *et al.*, 2014a-c; Liew *et al.*, 2014; Ferreira *et al.*, 2005; Ferreira *et al.*, 2006) for sandwich cylindrical panels with functionally graded core. In this study, we will examine the vibration behavior of FGM cylindrical sandwich panel using the Fourier series and state space technique. A few selected example problems of sandwich panels with aluminium/zirconia FGM core layer made of different materials are studied.

Theory and formulation: In this study, a simply supported cylindrical sandwich panel composed of metal and ceramic facing sheets and a host FGM core layer is considered. The panel has length L, span angle h_m, total thickness h, inner and outer radius r_i and r_o, respectively as depicted in Fig. 1. The Young's modulus and material density of the FGM core layer are assumed to vary according to the simple power-law along the radial direction:

$$E = E_0\left(\frac{r}{r_i + h_m}\right)^{m1};\ \rho = \rho_0\left(\frac{r}{r_i + h_m}\right)^{m2} \quad (1)$$
$$r_i + h_m \le r \le (r_0 - h_c)$$

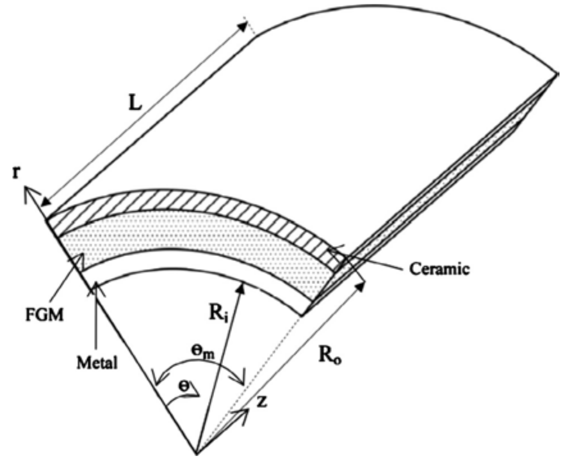

Fig. 1: Geometry of FGM sandwich panel

Where:

$$m_1\frac{\ln E_h/E_0}{\ln(r_0 - h_c)/r_i - h_m};\ m_2\frac{\ln\rho_h/\rho_0}{\ln(r_0 - h_c)/r_i - h_m}$$

The E_o, ρ_o, E_h, ρ_h are the Young's modulus and material density at the inner and outer surfaces of the FGM core layer, respectively. The equilibrium equation for the FGM core in cylindrical coordinate can be written in the form:

$$\begin{aligned}
&\frac{\partial\sigma_r}{\partial r} + \frac{\partial\sigma_{zr}}{\partial z} + \frac{1}{r}\frac{\partial\sigma_{r\theta}}{\partial\theta} + \frac{1}{r}(\sigma_r - \sigma_\theta) = \rho\frac{\partial^2 u}{\partial t^2}\\
&\frac{\partial\sigma_{r\theta}}{\partial r} + \frac{1}{r}\frac{\partial\sigma_\theta}{\partial\theta} + \frac{\partial\sigma_{\theta z}}{\partial z} + \frac{2}{r}(\sigma_{r\theta}) = \rho\frac{\partial^2 v}{\partial t^2} \qquad (2)\\
&\frac{\partial\sigma_{rz}}{\partial r} + \frac{1}{r}\frac{\partial\sigma_{\theta z}}{\partial\theta} + \frac{\partial\sigma_z}{\partial z} + \frac{\sigma_{rz}}{r} = \rho\frac{\partial^2 w}{\partial t^2}
\end{aligned}$$

where, τ_{ij} ($i = r, \theta, z$) are the normal and shear stress and u_i ($i = r, \theta, z$) are displacement components along the radial, circumferential and axial directions, respectively. Stress-displacement relations in linear elasticity are:

$$\begin{aligned}
&\sigma_r = \frac{E(r)}{(1+\gamma)(1-2\gamma)}\left[(1-\gamma)\frac{\partial u}{\partial r} + \frac{\gamma}{r}\left(\frac{\partial u_\theta}{\partial\theta} + u_r\right) + \gamma\frac{\partial w}{\partial z}\right]\\
&\sigma_\theta = \frac{E(r)}{(1+\gamma)(1-2\gamma)}\left[\gamma\frac{\partial u}{\partial r} + \frac{(1-\gamma)}{r}\left(\frac{\partial v}{\partial\theta} + u\right) + \gamma\frac{\partial w}{\partial z}\right]\\
&\sigma_z = \frac{E(r)}{(1+\gamma)(1-2\gamma)}\left[\gamma\frac{\partial u}{\partial r} + \frac{\gamma}{r}\left(\frac{\partial v}{\partial\theta} + u\right) + \frac{(1-\gamma)\partial w}{\partial z}\right] \qquad (3)\\
&\sigma_{z\theta} = \frac{E}{2(1+\gamma)}\left[\frac{\partial v}{\partial z} + \frac{1}{r}\frac{\partial w}{\partial\theta}\right]\\
&\sigma_{zr} = \frac{E}{2(1+\gamma)}\left[\frac{\partial w}{\partial r} - \frac{\partial u}{\partial z}\right]
\end{aligned}$$

$$\sigma_{r\theta}=\frac{E}{2(1+\gamma)}\left[\frac{1}{r}\frac{\partial u}{\partial\theta}+\frac{\partial v}{\partial r}-\frac{v}{r}\right] \quad (3)$$

The simply supported boundary conditions are expressed according to the following relations:

$$u_r=u_\theta=\sigma_z=0 \quad z=0,\ L \quad (4a)$$

$$u_r=u_z=\sigma_\theta=0 \quad \theta=0,\ \theta_m \quad (4b)$$

For free vibration analysis, the conditions on the inner and outer surface boundaries of the sandwich panel are assumed to be traction free:

$$\sigma_r=\sigma_{zr}=\sigma_{r\theta}=0 \quad r=r_i,\ r_o \quad (5)$$

MATERIALS AND METHODS

Analytical solution: The relations for simply supported boundary conditions, Eq. 4a and b are satisfied by the following Fourier series expansion of stress and displacement field:

$$\begin{aligned}
u&=\sum_{n=1}^{\infty}U\sin(p_n\theta)e^{i\omega t}\\
v&=\sum_{n=1}^{\infty}U\cos(p_n\theta)e^{i\omega t}\\
w&=\sum_{n=1}^{\infty}W\sin(p_n\theta)e^{i\omega t}\\
\sigma_r&=\sum_{n=1}^{\infty}\sigma'_r\sin(p_n\theta)\left(\frac{r}{r_i+h_m}\right)^{m_1}e^{i\omega t}\\
\sigma_\theta&=\sum_{n=1}^{\infty}\sigma'_\theta\sin(p_n\theta)\left(\frac{r}{r_i+h_m}\right)^{m_1}e^{i\omega t}\\
\sigma_z&=\sum_{n=1}^{\infty}\sigma'_z\sin(p_n\theta)\left(\frac{r}{r_i+h_m}\right)^{m_1}e^{i\omega t}\\
\sigma_{rz}&=\sum_{n=1}^{\infty}\sigma'_{rz}\sin(p_n\theta)\left(\frac{r}{r_i+h_m}\right)^{m_1}e^{i\omega t}\\
\sigma_{r\theta}&=\sum_{n=1}^{\infty}\sigma'_{r\theta}\cos(p_n\theta)\left(\frac{r}{r_i+h_m}\right)^{m_1}e^{i\omega t}\\
\sigma_{z\theta}&=\sum_{n=1}^{\infty}\sigma'_{z\theta}\cos(p_n\theta)\left(\frac{r}{r_i+h_m}\right)^{m_1}e^{i\omega t}
\end{aligned} \quad (6)$$

The physical quantities are: $U_i,\sigma'_i(i=r,\theta,z)$, $\sigma'_{rz},\sigma'_{r\theta},\sigma'_{z\theta}$ functions of r to be determined by satisfying equilibrium Eq. 2. Substituting Eq. 6 into Eq. 2 and 4 leads to the following equations:

$$\begin{aligned}
&\sigma'_{\tau_r}-\frac{p_m}{r}\tau'_{r\theta}-p_n\tau'_{xr}+\frac{1}{r}(m_1+1)\sigma'_\tau-\frac{\sigma'_\theta}{r}=\rho_0\omega^2U_r\left(\frac{r}{r_i+h_m}\right)^{m1}\\
&\sigma'_{r\theta,r}+\frac{p_m}{r}\sigma'_\theta-p_n\tau'_{z\theta}+\frac{1}{r}(m_1+2)r'_{zr}=-\rho_0\omega^2U_\theta\left(\frac{r}{r_i+h_m}\right)^{m1}\\
&\tau'_{zr,r}-\frac{p_m}{r}\tau_{r\theta}-p_n\sigma'_z+\frac{1}{r}(m_1+1)\tau'_{zr}=-\rho_0\omega^2U_z\left(\frac{r}{r_i+h_m}\right)^{m1}
\end{aligned} \quad (7)$$

And:

$$\begin{aligned}
\sigma'_r&=\frac{E(0)}{(1+\gamma)(1-2\gamma)}\left[(1-\gamma)U_{r,r}+\frac{\gamma}{r}(-p_mU_\theta+U_r)-\gamma p_nU_z\right]\\
\sigma_\theta&=\frac{E(0)}{(1+\gamma)(1-2\gamma)}\left[\gamma U_{r,r}+\frac{(1-\gamma)}{r}(-p_mU_\theta+U_r)-\gamma p_nU_Z\right]\\
\sigma_z&=\frac{E(0)}{(1+\gamma)(1-2\gamma)}\left[\gamma U_{r,r}+\frac{\gamma}{r}(-p_mU_\theta+U_r)-(1-\gamma)p_nU_z\right]\\
\tau'_{zr}&=\frac{E(0)}{2(1+\gamma)}\left[U_{z,r}+p_nU_r\right]\\
\tau'_{\theta r}&=\frac{E(0)}{2(1+\gamma)}\left[\frac{p_m}{r}U_r+U_{r,\theta}+\frac{U_\theta}{r}\right]\\
\tau'_{z\theta}&=\frac{E(0)}{2(1+\gamma)}\left[p_nU_\theta+\frac{p_m}{r}U_z\right]
\end{aligned} \quad (8)$$

The non-dimensional variables and elastic constants are introduced as follows:

$$(\bar\sigma_r\ \bar\sigma_\theta\ \bar\sigma_z\ \bar\tau_{zr}\ \bar\tau_{r\theta}\ \bar\tau_{z\theta})=\frac{\sigma'_r\ \sigma'_\theta\ \sigma'_z\ \sigma'_{zr}\ \sigma'_{\theta r}\ \tau')1}{E_m}$$

$$(\bar U_r\ \bar U_\theta\ \bar U_z)=(U_r\ U_\theta\ U_z)\frac{1}{h};\ h_m=\frac{h_m}{h},\ h_c=\frac{h_c}{h},\bar r=\frac{r}{R_m},\ \bar\theta=\frac{\theta}{\theta_m}$$

$$\bar P_n=LP_n,\quad \bar P_m=\theta_m,P_m,\ \bar Z=\frac{z}{L},\bar E_0=\frac{E_0}{E_m},\ \bar E_C\frac{E_C}{E_m} \quad (9)$$

Substituting Eq. 9 into Eq. 7 and 8, we obtain the following non-dimensional state space equation:

$$\frac{d\delta_f}{d\bar r}=G_f\delta_f \quad (10)$$

Where:

δ_f = $\{\bar\sigma_r\bar U_z\bar U_\theta\bar U_r\bar\sigma_{zr}\bar\sigma_{r\theta}\}^T$ are the state space variables

G_f = The square matrix of coefficients given in the Appendix 1

Since, the coefficient matrix G_f is not constant, it is difficult to solve Eq. 10 directly. It is possible to solve such differential equations by using the exponential series solutions as well as layer wise technique. In this study, we use the layer wise technique to divide the FGM layer into N fictitious thin layers. Thus, the coefficient matrix G_f can be assumed constant within each layer (denoted as Gf_k at the mid radius of the kth layer). Now, the general solution to Eq. 10 for kth layer of FGM is:

$$\delta_{fk}(r) = \delta_{ok} e^{G_{fk}(r + r_{K-1})} \bar{r}_{K-1} \leq \bar{r} \leq \bar{r}_k \quad \bar{r} = \bar{r}_{(k-1)} \tag{11}$$

$$r_k = r_i + h_m + \frac{k\bar{h}_f}{N};\ \delta_{fk}(\bar{r}_k) = M_{fk}\delta_{ok} \quad M_{fk} = \exp\left(G_{fk}\frac{\bar{h}_f}{N}\right) \tag{12}$$

by using continuity condition of the state variable at each fictitious interface, correlations between state variables at the inner and outer surfaces of the FGM core layer are derived:

$$\delta_{fh} = M_f \delta_0 \tag{13}$$

Where:

$$M_f = \Pi_{K=N}^{1} \exp\left(\frac{\bar{h}G_{fk}}{N}\right) \delta_0,\ \delta_{fk}$$

are the state vectors at the inner and outer surface of FGM layer, respectively. By substituting $m_1 = 0$ into Eq. 6 and 7 and using the same procedure as that used for the FGM layer, the related state space differential equations for the inner and outer facing layers, made of metal and ceramic, respectively, can be derived for the jth layer as follows:

$$\delta_{mj} = (\bar{r}) = \delta_{oj} e^{G_{my}(r - r_{j-1})} \ r_{j-1} \leq \bar{r} \leq \bar{r}_j \tag{14}$$

$$\bar{r}_{j-1} = \bar{r}_i + \frac{(j-1)\bar{h}_m}{M}$$

$$\bar{r}_{j-1} = \bar{r}_i + \frac{(j-1)\bar{h}_m}{M}$$

$$\bar{r}_k = \bar{r}_i + (j\bar{h}_m)/(M) \quad \delta_{oj} = \delta_{mj} \left| (\bar{r} = \bar{r}_{(k-1)})\right)$$

Where:

M = No. of fictitious layers

m = The metal

$$\delta_{cj}(r) = \delta_{oj} e^{G_{cj(\bar{r} - \bar{r}_{j-1})}} \ \bar{r}_{j-1} \leq \bar{r} \leq \bar{r}$$

Where:

$\bar{r}_{j-1}$ = $\mathbf{r_o + (m - j - 1)\bar{h}_c / M}$

r_j = $r_0 - ((m - j)\bar{h}_c / M\delta_{oj} = \boldsymbol{\delta}_{cj} \left| (r = (r_{(k-1)})\right.$

$\boldsymbol{\delta}_{oj}$ = $\delta_{cj} \left| (\bar{r} = (\bar{r}_{(k-1)})\right.$

c = The ceramic

Applying the continuity condition of the state variables at each fictitious interface for metal and ceramic layers yields the following correlations between state variables at the inner and outer surface of metal and ceramic facing sheets, respectively:

$$\delta_{mh} = M_m \delta_{om} \tag{15a}$$

$$\delta_{ch} = M_c \delta_{oc} \tag{15b}$$

Where:

$$M_m = \Pi_{j=m}^{1} \exp\left(\frac{h_m G_{mj}}{M}\right)$$

And:

$$M_c = \Pi_{j=m}^{1} \exp\left(\frac{h_m G_{cj}}{M}\right) \text{ and } \delta_{Ch},\ \delta_{mh},\ \delta_{Co}$$

The $\boldsymbol{\delta}_{mo}$ are the state vectors at the inner and outer surface of metal and ceramic layers, respectively. By using Eq. 13, 15a and 15b and noting that the state variables at the facing/core interfaces of the FGM sandwich panel are continuous, the following correlation between the state variables at the outer and the inner surfaces of the FGM sandwich panel is derived, i.e:

$$\delta(\bar{r}_0) = A\delta(\bar{r}_1) \tag{16}$$

where, $A = M_C T M_f M_m$. Imposing the surface traction free boundary conditions Eq. 5 in Eq. 16 leads to the following homogenous equations for displacement components at the inner surface of the sandwich panel:

$$\begin{bmatrix} A12 & A13 & A14 \\ A52 & A53 & A54 \\ A62 & A63 & A64 \end{bmatrix} \begin{bmatrix} U_z \\ U_\theta \\ U_r \end{bmatrix} = \begin{bmatrix} 0 \\ 0 \\ 0 \end{bmatrix} \tag{17}$$

Finally, a nontrivial solution to Eq. 17 leads to the characteristic equation for natural frequencies of the problem.

RESULTS AND DISCUSSION

In this study, numerical simulations are carried out for a simply-supported sandwich panel with aluminium/zirconia FGM core layer made of materials with the following properties:

$$E_m = E_0 = 70 GPa;\ \rho_m = \rho_0 = 2707 kg/k^3$$
$$E_c = E_h = 151 GPa;\ \rho_m = \rho_0 = 3000 kg/k^3$$

unless otherwise specified, values of other parameters are: $h_f = 20$ h; h = 0.1; s = $R_m/h = 10$; $\theta_m = \pi/4$.

The present formulation is first validated by comparing the numerical results to those reported values in the literature. As, there are no existing numerical results for three dimensional vibration of sandwich cylindrical panel with FGM core, the present formulation are simplified so as to compute results for the FGM cylindrical panel that can be compared with the available results by Bodaghi and Shakeri (2012) as listed in Table 1. In Table 1, a comparative study is carried out on the fundamental frequency of simply supported FGM cylindrical panel for various coefficients of power law, m_1. It is seen that the present results are in good agreement with reported results in Bodaghi and Shakeri (2012). It is noted that the discrepancy is due to the conventional two-dimensional first-order shear deformation theory which was used in (Zhang *et al*., 2012). For further discussion, numerical investigations are carried out. The results are presented in Table 2-3 and Fig. 1-3. Influence of the number of circumferential and axial modes on the first dimensionless frequency for various circumferential dimensions θ_m is listed in Table 2.

From Table 2, it is observed that dimensionless frequency increases when the number of circumferential modes and axial modes increases. It can be concluded that variation of the circumferential dimension has more effect on the axial mode of vibration than the circumferential mode. Table 3 presents the effect of the number of circumferential modes (m) on the first three non-dimensional natural frequencies of thin and thick sandwich cylindrical panels. As, it can be seen from Table 3, the effect of m on the natural frequencies is more pronounce in the higher frequencies than in the lower frequencies. It can be further concluded that the influence of the number of circumferential modes in thick panel is more significant. The influence of FGM core layer thickness to the facing layer thickness ratio on the non-dimensional fundamental frequency is depicted in Fig. 2. From Fig. 2, it can be seen that increase the thickness of the FGM layer up to nearly $h_{fc}/h_m = 20$ causes significant increase in the fundamental frequency. The rate decreases until the thickness ratio reaches $h_{fc}/h_m = 120$ The stiffness of the sandwich panel increases when the FGM layer thickness increases and consequently, the fundamental frequency of the panel increases. The effect of L/R_m on the dimensionless fundamental frequency of thick and thin sandwich cylindrical FGM panels is depicted in Fig. 3. The stiffness of panel decreases when the length to mid-radius ratio increases which results in decrease in the fundamental frequency parameter. It can also been seen that this effect is significant when the length to mid-radius ratio is <2. When, the length to mid-radius ratio is >2, the effect decreases when the length to mid-radius ratio increases up to nearly L/R_m after which the effect can be ignored. Moreover, it can be concluded that the maximum length to mid-radius ratio

Table 1: Comparison of the dimentionless fundamental frequency for the simply supported FG cylindrical panel

		m_1			
R_m/L	Methods	0	0.5	1	2
0.5	Ref.(30)	70.0540	60.5121	54.9027	48.7172
	Presen	70.0900	60.5710	54.9620	48.7802
1	Ref.(30)	52.1831	43.8018	39.2122	34.7501
	Presen	52.1991	43.8680	39.2760	34.798
5	Presen	42.6550	35.0092	30.7008	27.5511
	Ref.(30)	42.6589	35.0343	30.7304	27.5802
10	Presen	42.3000	34.6999	30.7008	27.3138
	Ref.(30)	42.3502	34.7201	30.7305	27.3402

Table 2: Effect of circumferential dimension, θm on the non-dimensional first natural frequency of the sandwich cylindrical panel for the various circumferential and axial modes number

		N				
θ_m	M	1	2	3	4	5
π/2	1	0.829	1.792	3.102	4.765	6.6690
	2	1.461	2.374	3.704	5.338	7.1940
	3	2.762	3.545	4.759	6.291	8.0520
	4	4.397	5.084	6.168	7.566	9.2020
	5	6.251	6.858	7.824	9.089	10.593
2π/3	1	0.716	1.742	3.003	4.660	6.5710
	2	1.113	1.908	3.251	4.912	6.8060
	3	1.461	2.374	3.704	5.338	7.1940
	4	2.283	3.104	4.362	5.934	7.7310
	5	3.277	4.025	5.195	6.684	8.4050
2π/6	1	0.608	1.734	2.969	4.624	6.5370
	2	1.011	1.792	3.103	4.765	6.6690
	3	1.121	1.996	3.344	5.002	6.8880
	4	1.461	2.374	3.704	5.338	7.1940
	5	2.059	2.901	4.18	5.770	7.5830
	1	0.503	1.733	2.954	4.607	6.5210
	2	0.862	1.755	3.037	4.697	6.6060
	3	1.001	1.853	3.185	4.848	6.7460
	4	1.108	2.058	3.407	5.062	6.9430
	5	1.461	2.374	3.704	5.338	7.1940

Table 3: Effect of circumferential mode number, m, on first three non-dimensional natural frequency of the thin sandwich cylindrical panel for n = 1

S	M	ω_1	ω_2	ω_3
5	1	1.508	3.807	6.4200
	2	3.668	6.301	10.550
	3	6.395	9.057	14.327
10	1	0.913	3.79	6.4510
	2	2.283	6.289	10.816
	3	4.397	11.88	19.966
30	1	0.519	3.78	6.4400
	2	0.851	6.286	10.858
	3	1.75	9.053	15.623

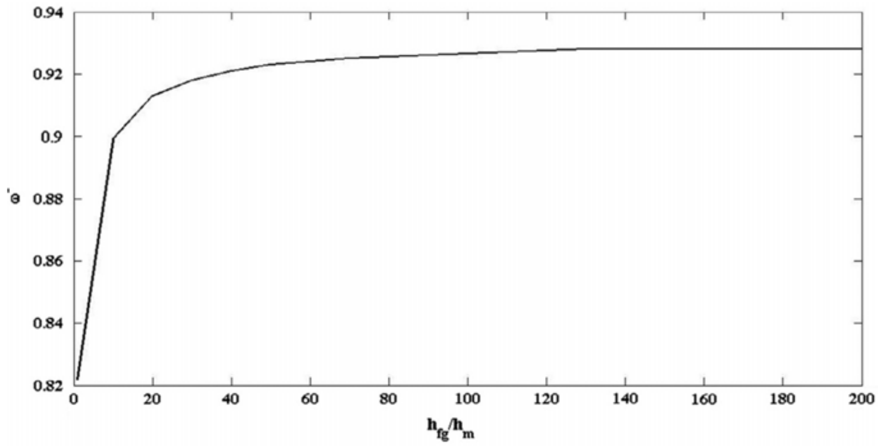

Fig. 2: Effect of FGM to metal thickness ratio on the non-dimensional fundamental frequency of sandwich cylindrical FGM panel with S = 10, h = 10, L = Rm, m = n = 1, θm = π/4

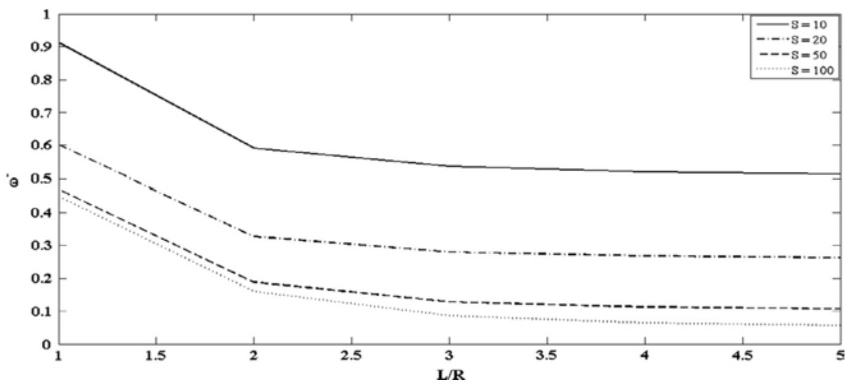

Fig. 3: Effect of L/R_m on dimensionless fundamental frequency of thick and thin sandwich cylindrical FGM panel

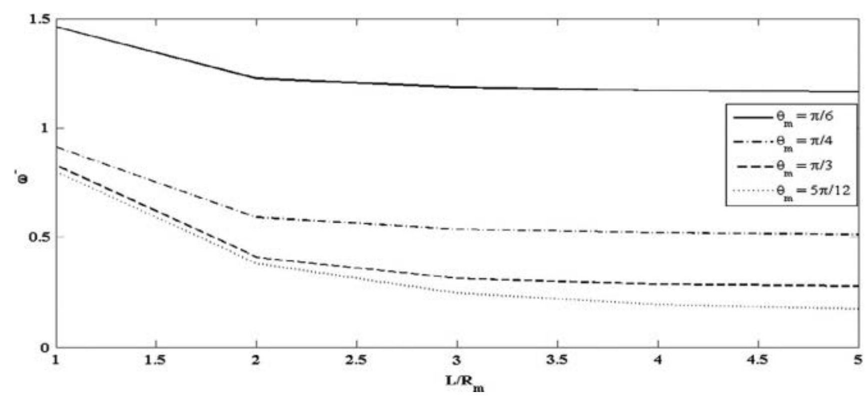

Fig. 4: Effect of L/R_m on dimensionless fundamental frequency of sandwich cylindrical FGM panel with various circumferential dimension and m = n = 1

which does not affect the fundamental frequency in thick panel is smaller than that in thin panel. Figure 4 depicts the effect of L/R_m on the dimensionless fundamental frequency of sandwich cylindrical FGM panel with various circumferential dimensions. As shown in the figure, increase in the circumferential dimension m θ_m, the stiffness of the panel decreases which results in decrease in the dimensionless fundamental frequency. Besides, it is observed that the effect of length to mid-radius ratio on the fundamental frequency parameter depends directly on the circumferential dimension.

Simulation: After this procedure, simulation of this panel in ABAQUS Software is possible and we can get more

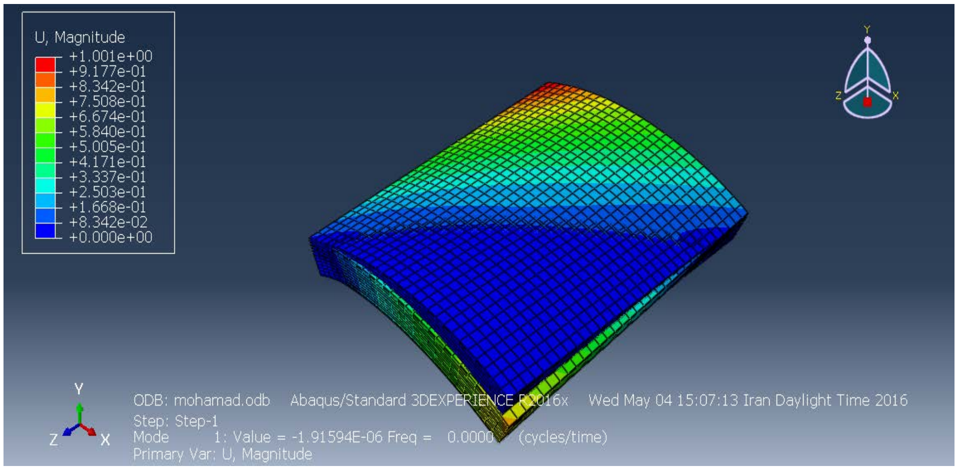

Fig. 5: First mode of vibration in ABAQUS Software

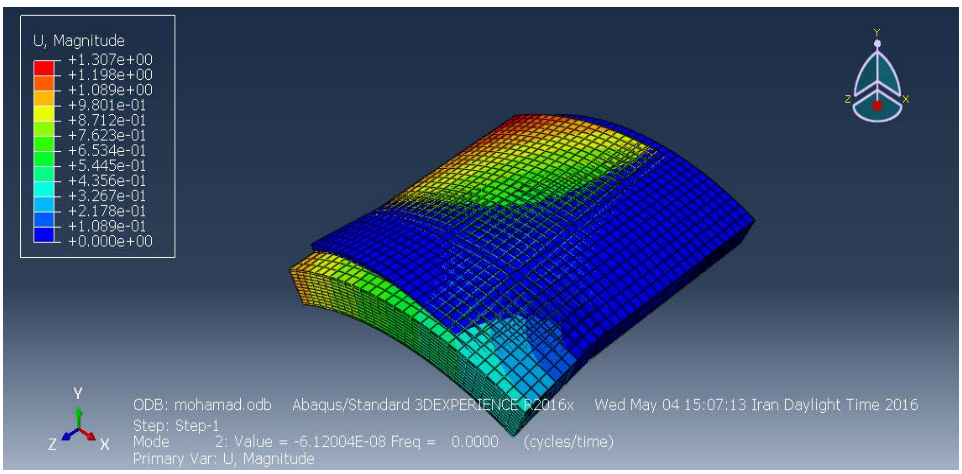

Fig. 6: Second mode of vibration in ABAQUS Software

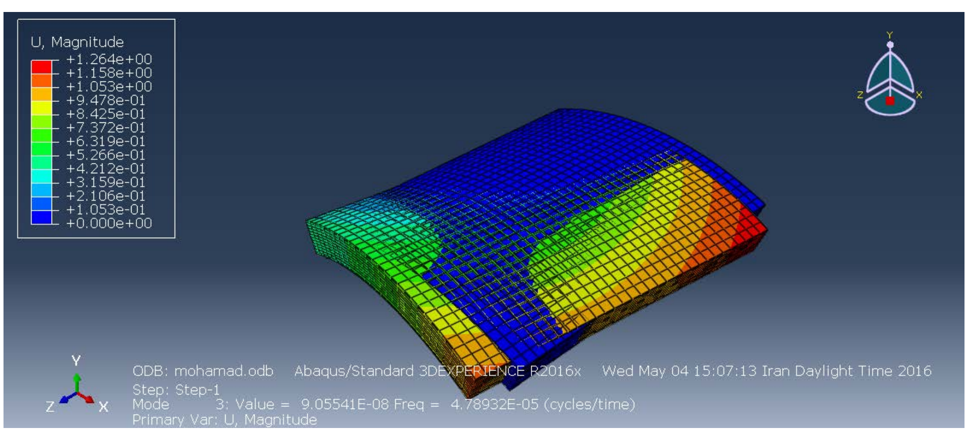

Fig. 7: Third mode of vibration in ABAQUS Software

information and output after this way. We considered FGM layer to 10 layer and property of each layer has changed through the thickness. Formulation solved by Maple Software and we get the specific modulus of elasticity for each layer. As you can see from Fig. 4-9, these are modes of vibration.

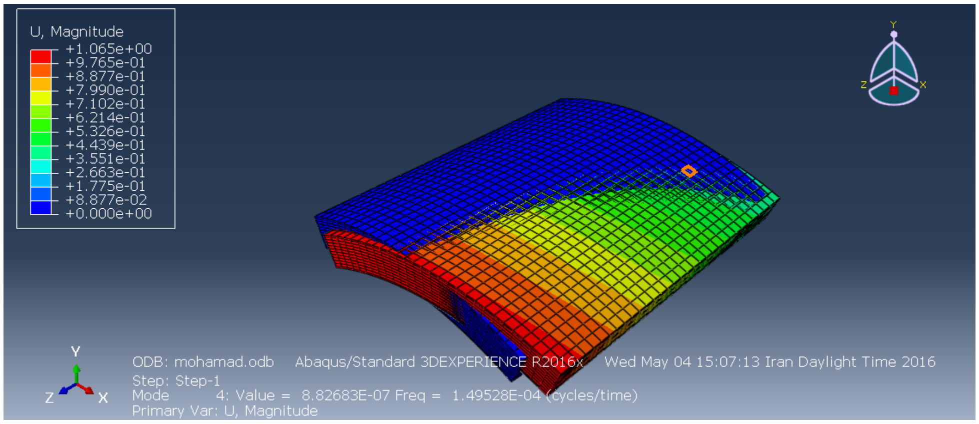

Fig. 8: Fourth mode of vibration in ABAQUS Software

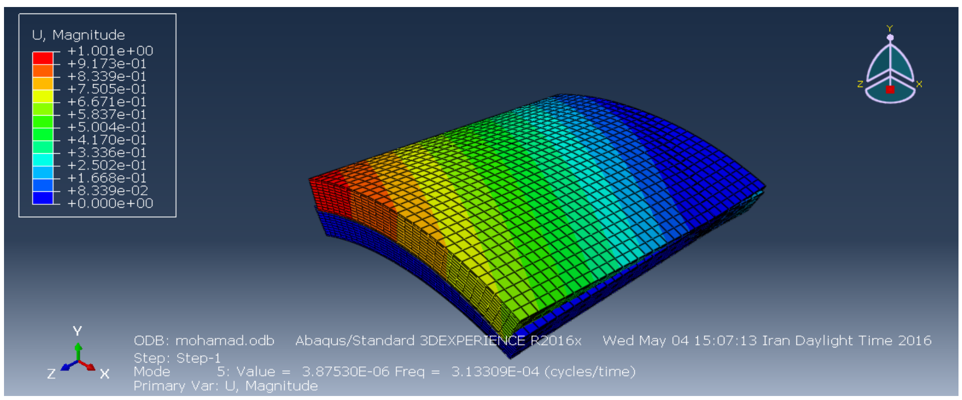

Fig. 9: Fifth mode of vibration in ABAQUS Software

CONCLUSION

Based on the theory of elasticity, a first known exact free vibration solution of simply supported FGM sandwich cylindrical panel was presented. A coupled technique, using the Fourier series expansion along the axial and circumferential directions and state space technique in the radial direction, was used to obtain the solution. A comparison study was carried out to validate the accuracy of the present formulation. The exact vibration solution obtained from the present method can be used as a benchmark reference for assessing the validity of newly developed numerical techniques for approximate solution of sandwich cylindrical panels with functionally graded core. In this study, the numerical illustrations have revealed that: circumferential dimension has significant effect on the axial mode of vibration than the circumferential mode of vibration:

- Effect of the number of circumferential modes in the thick panel is more significant
- Difference between the first three natural frequencies decreases when the circumferential mode number increases
- FGM layer thickness to facing thickness ratio affects the vibration behavior of the sandwich panel more pronounce at the lower ratio; however, after the ratio increases up to a specified value, the influence of the facing layer can be neglected
- The frequency behavior is affected by the length to mid-radius ratio strongly when $L/R_m<2$
- Maximum length to mid-radius ratio does not affect the fundamental frequency in the thick panel than that in the thin panel
- The fundamental frequency at a specified S for the metal/FGM/ceramic layup is always greater than that for other layups
- The effect of S on the first natural frequency of the higher mode is more significant
- The influence of S on the first natural frequency of each mode in the thick panel is more significant than that for the moderately thick panel
- The numerical result and simulation result has good correlation

APPENDIX 1

$$G_f = [(A_1 \; A_2 \; A_3 \; A_4 \; P_n R_{m/L} \; R_{m/r}$$
$$1/\theta_m @ 0 \; 0 \; 0 \; P_n R_{m/L} \; A_5 \; 0 \; 0 \; 0]$$

Where:

$$A_1 = \frac{1}{\bar{r}}\left[\left(\frac{r}{1-\gamma} - 1 + m_1\right)\right]$$

$$A_2 = \frac{1}{\bar{r}}\left(\frac{h}{L}\right)\left(\frac{\bar{E}_0 \gamma \bar{P}_n}{(1-\gamma^2)}\right)\frac{E_0}{(1-\gamma^2)}$$

$$A_5 = \frac{Z(1+\gamma)}{\bar{E}_0}\left(\frac{R_m}{h}\right)$$

$$A_6 = \frac{(1+\gamma)(1-2\gamma)}{\bar{E}_0(1-\gamma)}\left(\frac{R_m}{h}\right)$$

$$A_7 = \frac{\gamma P_n}{(1-\gamma)}\left(\frac{R_m}{L}\right)$$

$$A_8 = \frac{\gamma P_m}{r\theta_m(1-\gamma)}$$

$$A_9 = \frac{E_0}{(1-\gamma)}\left(\frac{h R_m}{L^2}\frac{\bar{P}_n^2}{1-\gamma} + \frac{h}{R_m \theta_m^2}\frac{\bar{p}_n^2}{Z \bar{r}^2}\right)$$

$$A_{10} = \frac{P_n P_m \bar{E}_0}{2\bar{r}(1-\gamma)}\left(\frac{h}{L}\right)\frac{1}{\theta_m}$$

$$A_{11} = \frac{-p_n \gamma E_0}{r(1-\gamma^2)}\left(\frac{h}{L}\right)$$

$$A_{12} = \frac{E_0}{(1-\gamma)}\left(\frac{h R_m}{L^2}\frac{P_n}{Z(1+\gamma)} + \frac{h}{R_m \theta_m^2}\frac{p^{-2}}{r^{-2}(1-\gamma)}\right)\bar{r}_0 \bar{h}$$

REFERENCES

Alibeigloo, A. and A.M. Kani, 2010. 3D free vibration analysis of laminated cylindrical shell integrated piezoelectric layers using the differential quadrature method. Applied Math. Mod., 34: 4123-4137.

Alibeigloo, A., 2011. Free vibration analysis of nano-plate using three-dimensional theory of elasticity. Acta Mech., 222: 149-159.

Alibeigloo, A., 2012. Three-dimensional free vibration analysis of multi-layered graphene sheets embedded in elastic matrix. J. Vibration Control, 19: 2357-2371.

Alibeigloo, A., 2014. Free vibration analysis of functionally graded carbon nanotube-reinforced composite cylindrical panel embedded in piezoelectric layers by using theory of elasticity. Eur. J. Mech. A/Solids, 44: 104-115.

Alibeigloo, A., A.M. Kani and M.H. Pashaei, 2012. Elasticity solution for the free vibration analysis of functionally graded cylindrical shell bonded to thin piezoelectric layers. Int. J. Pressure Vessels Piping, 89: 98-111.

Aragh, B.S. and M.H. Yas, 2011. Effect of continuously grading fiber orientation face sheets on vibration of sandwich panels with FGM core. Int. J. Mech. Sci., 53: 628-638.

Biglari, H. and A.A. Jafari, 2010. High-order free vibrations of doubly-curved sandwich panels with flexible core based on a refined three-layered theory. Comp. Struct., 92: 2685-2694.

Bodaghi, M. and M. Shakeri, 2012. An analytical approach for free vibration and transient response of functionally graded piezoelectric cylindrical panels subjected to impulsive loads. Comp. Struct., 94: 1721-1735.

Chakrabarti, A. and R.K. Bera, 2002. Nonlinear vibration and stability of a shallow unsymmetrical orthotropic sandwich shell of double curvature with orthotropic core. Comput. Math. Applic., 43: 1617-1630.

Dozio, L., 2013. Natural frequencies of sandwich plates with FGM core via variable-kinematic 2-D Ritz models. Comp. Struct., 96: 561-568.

Ferreira, A.J.M., R.C. Batra, C.M.C. Roque, L.F. Qian and P.A.L.S. Martins, 2005. Static analysis of functionally graded plates using third-order shear deformation theory and a meshless method. Comp. Struct., 69: 449-457.

Ferreira, A.J.M., R.C. Batra, C.M.C. Roque, L.F. Qian and R.M.N. Jorge, 2006. Natural frequencies of functionally graded plates by a meshless method. Comp. Struct., 75: 593-600.

Gipson, G.S., 1989. Determinantal Rayleigh-Ritz expressions for natural frequencies of sandwich panels with orthotropic face plates. Math. Comput. Mod., 12: 169-180.

Kashtalyan, M. and M. Menshykova, 2009. Three-dimensional elasticity solution for sandwich panels with a functionally graded core. Comp. Struct., 87: 36-43.

Khare, R.K., T. Kant and A.K. Garg, 2004. Free vibration of composite and sandwich laminates with a higher-order facet shell element. Comp. Struct., 65: 405-418.

Kumar, A., A. Chakrabarti and P. Bhargava, 2013. Vibration of laminated composites and sandwich shells based on higher order zigzag theory. Eng. Struct., 56: 880-888.

Liew, K.M., Z.X. Lei, J.L. Yu and L.W. Zhang, 2014. Postbuckling of carbon nanotube-reinforced functionally graded cylindrical panels under axial compression using a meshless approach. Comput. Methods Applied Mech. Eng., 268: 1-17.

Mohammadi, F. and R. Sedaghati, 2012. Linear and nonlinear vibration analysis of sandwich cylindrical shell with constrained viscoelastic core layer. Int. J. Mech. Sci., 54: 156-171.

Moreira, R.A.S. and J.D. Rodrigues, 2010. Static and dynamic analysis of soft core sandwich panels with through-thickness deformation. Comp. Struct., 92: 201-215.

Neves, A.M.A., A.J.M. Ferreira, E. Carrera, M. Cinefra, C.M.C. Roque, R.M.N. Jorge, C.M.M. Soares, 2013. Static, free vibration and buckling analysis of isotropic and sandwich functionally graded plates using a quasi-3D higher-order shear deformation theory and a meshless technique. Comp. Part B: Eng., 44: 657-674.

Rahmani, O., S.M.R. Khalili and K. Malekzadeh, 2010. Free vibration response of composite sandwich cylindrical shell with flexible core. Comp. Struct., 92: 1269-1281.

Singh, A.V., 1999. Free vibration analysis of deep doubly curved sandwich panels. Comput. Struct., 73: 385-394.

Sobhy, M., 2013. Buckling and free vibration of exponentially graded sandwich plates resting on elastic foundations under various boundary conditions. Compos. Struct., 99: 76-87.

Xia, Z.Q. and S. Lukasiewicz, 1995. Non-linear analysis of damping properties of cylindrical sandwich panels. J. Sound Vibration, 186: 55-69.

Yas, M.H., A. Pourasghar, S. Kamarian and M. Heshmati, 2013. Three-dimensional free vibration analysis of functionally graded nanocomposite cylindrical panels reinforced by carbon nanotube. Mater. Design, 49: 583-590.

Zhang, L.W., Y.J. Deng and K.M. Liew, 2014a. An improved element-free Galerkin method for numerical modeling of the biological population problems. Eng. Anal. Boundary Elements, 40: 181-188.

Zhang, L.W., Z.X. Lei, J.L. Yu and K.M. Liew, 2014b. Static and dynamic analysis of carbon nanotube reinforced composite cylindrical panels. Comp. Struct., 111: 205-212.

Zhang, L.W., P. Zhu and K.M. Liew, 2014c. Thermal buckling of functionally graded plates using a local Kriging meshless method. Compos. Struct., 108: 472-492.

Zhu, P., L.W. Zhang and K.M. Liew, 2014. Geometrically nonlinear thermomechanical analysis of moderately thick functionally graded plates using a local Petrov-Galerkin approach with moving Kriging interpolation. Compos. Struct., 107: 298-314.